Digest Journal of Nanomaterials and Biostructures

*Dig. J. Nanomater. Bios.* **2026**; 21(2): 55319
https://doi.org/10.31083/DJNB55319

*Original Research*

# Green Synthesis of Silver Nanoparticles Using *Zanthoxylum Fagara* L. Sarg Leaf Extract and Assessment of Their Photocatalytic Degradation Performance

Laith Saleh Alhiti[1,*], Ruqaya Talib Kadhim[2], Ibtihaj Hussein Ali[3]

[1]Medical Physics Department, University of Anbar, 31007 Anbar, Iraq
[2]Ministry of Education, General Directorate for Education in Thi-Qar, 64001 Thi Qar, Iraq
[3]Ministry of Education, General Directorate for Education in Al- Qadisiyah, 58001 Al-Diwaniyah, Iraq
*Correspondence: laith2011alhiti@uoanbar.edu.iq (Laith Saleh Alhiti)
Academic Editor: Giuseppe Trusso Sfrazzetto
Submitted: 11 January 2026 Revised: 30 March 2026 Accepted: 7 April 2026 Published: 26 June 2026

**Abstract**

The plant material–mediated synthesis of silver nanoparticles (AgNPs) has drawn considerable attention because of its green nature and cost-effectiveness. Herein, we prepared AgNPs using *Zanthoxylum fagara* L. Sarg. leaf extract at different temperatures (50, 60, 70, and 80 °C) and investigated their structural, morphological, and photocatalytic properties using ultraviolet–visible (UV–Vis) spectroscopy, Fourier transform infrared (FTIR) spectroscopy, X-ray diffraction (XRD), atomic force microscopy (AFM), and scanning electron microscopy (SEM). Photocatalytic performance was quantified in terms of methylene blue (MB) removal efficiency under irradiation (5–60 min). AgNPs synthesized at 70 °C exhibited the highest apparent removal efficiency after 60 min. UV–Vis measurements indicated that the apparent MB removal was due to decolorization and not absolute mineralization. This process was termed apparent degradation. Our findings imply that the synthesized AgNPs are well suited for dye decolorization in aqueous media. FTIR spectroscopy revealed the presence of AgNP-stabilizing functional groups. XRD analysis showed that AgNPs were crystalline in nature, and AFM and SEM showed that the spherical-shaped AgNPs and average diameter of the nanoparticles increased with increasing temperature. Our results show that *Zanthoxylum fagara* L. Sarg. leaf extract is an efficient reducing and stabilizing agent for AgNP production and reveals the important role of temperature in regulating the nanoparticle size and morphology, which directly influence photocatalytic behavior. Although AgNPs showed good prospects for environmental remediation practices, their quantum efficiency, extent of mineralization, and reusability were not explored and should be examined in the future to further consider environmental applicability.

**Keywords:** nanotechnology; green method; silver nanoparticles; water quality; waste; photocatalytic degradation

## 1. Introduction

Recent global estimates of nanotechnology markets show that silver nanoparticles (AgNPs) are among the fastest-growing classes of engineered nanomaterials, largely because of their broad technological, environmental, and biomedical applications [1]. Silver nanoparticles are typically defined as metallic silver structures with at least one dimension smaller than 100 nm, a scale at which their physicochemical behavior differs significantly from that of bulk silver due to the intense quantum size effects and high surface-to-volume ratio observed in this regime [2]. It is precisely this nanoscale regime in which the new optical, catalytic, and biological properties emerge in AgNPs that make them useful in the current antimicrobial systems (plasmonic) sensing technologies, water remediation technology, and photocatalytic degradation technology [3]. Generally, it is possible to distinguish between two types of methods used in the synthesis of silver nanoparticles. There are top-down physical and bottom-up chemical and biological reduction approaches [4]. Top-down physical methods include laser ablation [5], thermal evaporation [6], arc discharge, and mechanical milling. Such processes involve complex equipment, whether with high energy input or costly operating conditions [7]. The chemical or biological reductions that represent bottom-up strategies include primarily silver ions, which are reduced to metallic $Ag^0$ atoms [8], which then further nucleate and develop into nanosized clusters stabilized by various capping agents [9]. Although classical chemical reduction routes, including citrate reduction (Turkevich method), borohydride reduction [10], and Tollens' reaction, provide controllability, they involve hazardous reagents with potential environmental risks and pose challenges in biocompatibility [11].

Green synthesis has emerged due to the inadequacy of traditional physical and chemical methodologies [12]. Therefore, green synthesis, or the reduction and stabilization of metal ions by biological systems such as bacteria [13], fungi, algae, and plants, mainly under mild conditions, which are inexpensive as well as friendly to the environment, has been defined [14]. The extreme interest in plant-mediated synthesis is justified by the fact that botanical extracts contain a high diversity of biomolecules, including polyphenols, flavonoids, alkaloids, terpenoids, phenolic acids, vitamins, and antioxidants [15], which may act naturally and synergistically as reducing, capping, and stabilizing agents [16]. Many studies have reported multifunc-

tional catalytic [17], antimicrobial [18], and environmental pollutant removal [19] relevant properties of morphologically controlled highly stable colloidal plant-derived AgNPs [20].

*Zanthoxylum fagara* L. Sarg. is rich in phenolic compounds, alkaloids, essential oils, and antioxidants. It has recently been identified as a potential medicinal plant for the green synthesis of metallic nanoparticles with strong bioreductive properties [21]. The phytochemical richness of *Zanthoxylum fagara* L. Sarg. implies its high potential to facilitate the rapid reduction of $Ag^+$ ions while stabilizing the formed nanostructures by surface passivation. There are very few reports on silver nanoparticles synthesized using *Zanthoxylum fagara* L. Sarg. extract (Zf-AgNPs), and none have reported their catalytic activity in the photocatalytic degradation of organic pollutants, in which large areas remain unexplored [22].

Dye pollutants from the textile, paper, pharmaceutical, food, and plastic industries are persistent contaminants in aquatic environments because of their toxicity, chemical stability, and resistance to biodegradation [23]. An advanced yet sustainable method for dye remediation is photocatalytic degradation, in which AgNPs act as efficient catalysts through their surface plasmon resonance (SPR) effect, which enhances electron–hole separation, with consequent reactive oxygen species capable of mineralizing dye molecules [24]. With a global interest in eco-engineered nanomaterials for wastewater treatment, an assessment of the photocatalytic efficiency of *Zanthoxylum fagara* L. Sarg.-derived AgNPs introduces both scientific and environmental values. Therefore, this study involves the green synthesis of silver nanoparticles from an aqueous extract of *Zanthoxylum fagara* L. Sarg. and a detailed structural, optical, and morphological characterization besides reporting for the first time the catalytic pathways in detail; degradation kinetics; environmental applications as well as potential application wherein photocatalytic activity against an organic model dye by newly synthesized AgNPs has been explored. The limited research that has been conducted on *Zanthoxylum fagara* L. Sarg. extracts in the nanoparticle synthesis process and its possible application in photocatalytic dye degradation has not been performed in depth.

## 2. Materials and Methods

Fresh leaves of *Zanthoxylum fagara* L. Sarg. were obtained from a cultivated farm in a city known as Hit, Anbar Governorate, Iraq. Plant material was thoroughly washed with distilled water to remove surface impurities and dried at room temperature before use. All experiments were conducted using analytical-grade silver nitrate ($AgNO_3$, purity 99%, Lot No. SLCD9485, Sigma Aldrich, St. Louis, MO, USA) and deionized water without additional purification. The chemicals used in this study were of high purity and were used as received.

Laith Saleh Alhiti (Department of Medical Physics, College of Applied Sciences -Hit, University of Anbar, Anbar Governorate, Iraq) provided the data for the experiment and study design.

### *2.1 Preparation of Plant Extract*

The extraction conditions in this study were chosen based on the aqueous extraction conditions usually reported for the synthesis of plant-mediated nanoparticles. The solid-to-liquid ratio (3 g fresh leaves in 100 mL of distilled water) was set to guarantee adequate extraction of water-soluble phytochemicals, including polyphenols, flavonoids, alkaloids, and proteins, which are reported to be involved in the reduction and stabilization of metal nanoparticles [25]. Extraction temperatures in the range of extraction temperatures (70–80 °C) was used to maximize the release of bioactive compounds in plant tissues and reduce the potential for degradation of the bioactive compounds by heating. The extract was then stored at a low temperature (approximately 3 °C) after filtration to reduce enzymatic action and maintain the stability of the phytochemical components before the preparation of nanoparticles. Such extraction conditions have been extensively employed in earlier experiments in which plant-mediated syntheses of metallic nanoparticles were performed under the same conditions, as shown in Fig. 1 [26].

### *2.2 Preparation of Silver Nanoparticles (AgNPs)*

Silver nanoparticles were produced at different temperatures. To determine how temperature affects the development of silver nanoparticles, a one-factor-at-a-time study was performed, in which the temperature was manipulated, and other parameters of the synthesis process, such as the concentration of silver nitrate, extract volume, and reaction time, were held constant. This approach was used to separate the influence of temperature on the reduction dynamics of $Ag^+$ ions and the nucleation and growth mechanisms of AgNPs. To ensure the consistency of the experiment and better understand the impact of each parameter, it is a widespread practice in research on the synthesis of nanoparticles using plants to keep the reaction conditions constant.

Once the plant extract was made, 2 mL of the solution was transferred into 18 mL of a solution of 1 mM silver nitrate and stirred. The solution was stirred at 500 rpm and left to stand at reaction temperatures of 50, 60, 70, and 80 °C for 30 min. After 20 min of adding the leaf extract of a plant named *Zanthoxylum fagara* L. Sarg. The solution turned pale yellow, which slowly changed to a dark hue, indicating the rapid development of AgNPs. The mixture was left on a magnetic stirrer for 45 min, as shown in Fig. 2. The sample was then purified by centrifugation using a centrifuge at 5000 rpm for 30 min. The resulting AgNPs were centrifuged thrice. The precipitate of the silver nanoparticles was placed in clean glass vials. This process was repeated at 50, 60, 70, and 80 °C [27].

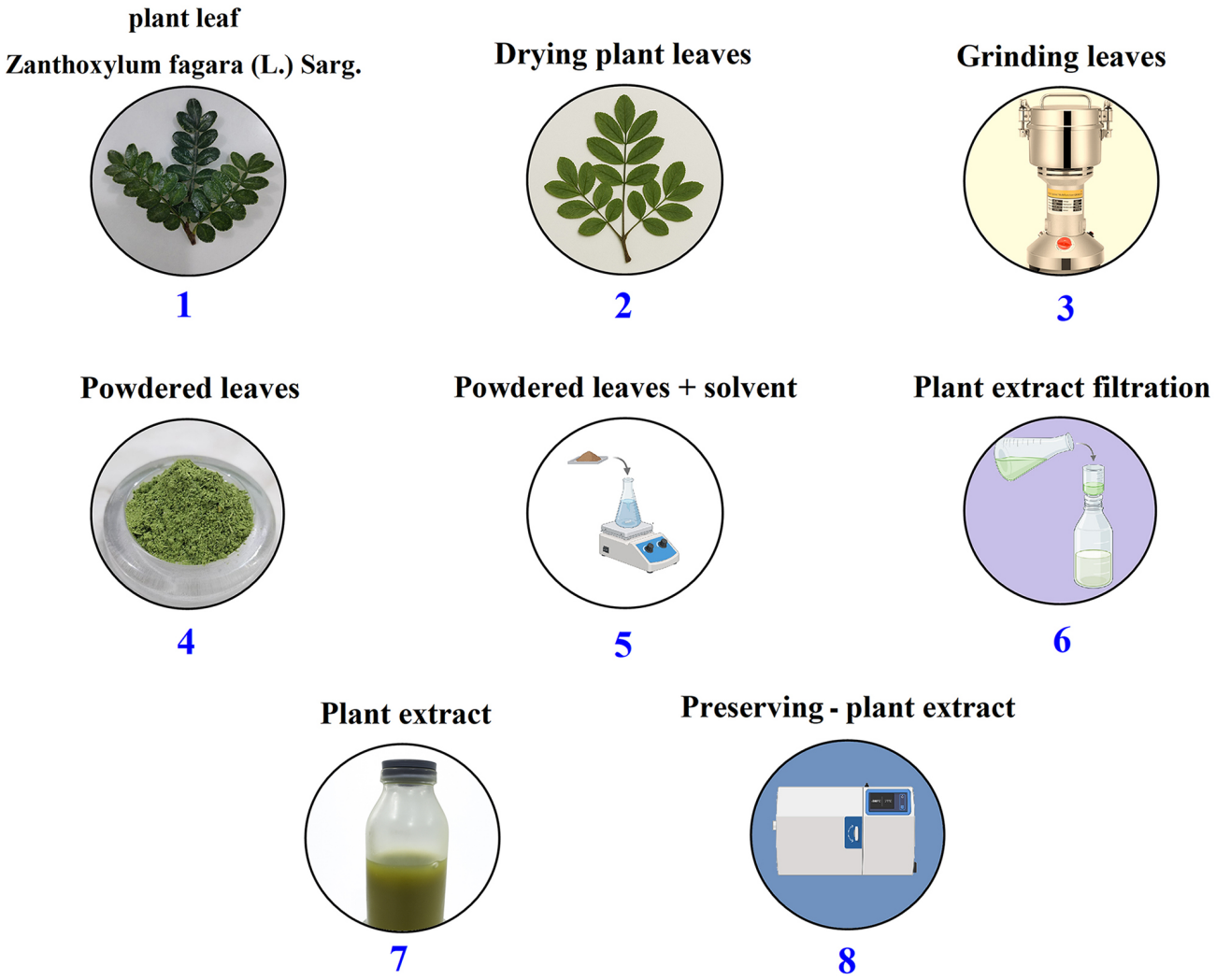


**Fig. 1. Method of preparing the aqueous plant extract of *Zanthoxylum fagara* L. Sarg. leaves.**

## 3. Results

### *3.1 Ultraviolet–Visible Spectroscopy (UV–Vis)*

The UV–Vis (UV-1900i, Shimadzu C., Kyoto, Japan. College of Applied Sciences - Hit / University of Anbar, Iraq) extinction spectra of the colloidal Ag nanoparticles synthesized at 50, 60, 70, and 80 °C exhibit a single, well-defined localized surface plasmon resonance (LSPR) band [28] with maxima at 415, 418, 420, and 422 nm, respectively, and peak absorbances of 1.35, 1.60, 1.80, and 2.45 a.u, as shown in Figs. 3,4. The LSPR band progressively red shifts and increases in intensity with increasing synthesis temperature; the highest-temperature sample (80 °C) also shows a modest increase in full width at half-maximum (FWHM) and a raised baseline at short wavelengths [29,30].

The observed LSPR behavior is consistent with temperature-dependent changes in the nanoparticle physical parameters that govern the plasmon resonance [31], particle size, size distribution (polydispersity), interparticle coupling (aggregation), and local dielectric environment [32]. A red-shift of the dipolar plasmon peak ($\Delta\lambda \approx 7$ nm, from 50 → 80 °C) together with an increase in extinction is most readily explained by an increase in the characteristic particle dimension and/or the formation of small aggregates at higher synthesis temperatures. For silver nanoparticles, an increase in the mean diameter produces a longer wavelength plasmon owing to retardation and multipolar contributions, yielding a larger extinction cross-section per particle. Partial aggregation or reduced interparticle spacing produces plasmon coupling, which red-shifts and broadens the resonance. The modest broadening of the band at 80 °C further indicates increased polydispersity or the appearance of nonspherical (anisotropic) morphologies, which introduce additional plasmon modes and inhomogeneous broadening [32].

### *3.2 Fourier Transform Infrared Spectroscopy (FTIR)*

FTIR was used to detect the presence of functional groups in the plant extract and to identify the molecular species that reduced and stabilized AgNPs [33]. The FTIR spectra of the crude extract and biosynthesized AgNPs showed several discrete vibrational bands that pro-


**Fig. 2. Silver nanoparticle solution synthesized by the green method at, 50 °C, 60 °C, 70 °C, 80 °C.**

vided information on the chemical changes that occurred during the formation of the nanoparticles [34]. FTIR spectroscopy is a well-known method used to identify the characteristic vibrational bands of phytochemicals, such as hydroxyl, carbonyl, amine, and phenolic groups, which are present in the plant medium used for the production of metal nanoparticles in green synthesis [35]. These functional groups are generally present in plant-derived compounds, such as polyphenols, flavonoids, alkaloids, and proteins, and are known to be natural reducing and capping groups in nanoparticle formation. Thus, the mechanistic explanation of the present study rests on the recognition of these functional groups using FTIR spectra and their previously known functions in the literature, as opposed to the description of chromatographic profiling of the plant extract. This strategy has gained popularity in various studies that examine the synthesis of metallic nanoparticles using plants [36].

In the FTIR spectrum of the plant extract, characteristic absorption bands were observed at approximately 560, 1127, and 1620 $cm^{-1}$, as shown in Fig. 5. The band at approximately 560 $cm^{-1}$ is normally attributed to the out-of-plane bending vibrations of aromatic rings or metal-oxygen bond straight stretching of foreign chemical residues. The Observed C–O–C and C–O stretching vibrations were at 1127 $cm^{-1}$, which are indicative of polysaccharides, flavonoids and other oxygenated vital constituents. The peak at 1620 $cm^{-1}$ is sharp and may represent the C=O functional group of amides or C=C functional group of aromatics and indicates that proteins, polyphenols, and other reducing agents might be present which may undergo an oxidation process [37]. When AgNPs were formed, significant spectral variations were observed. The FTIR spectrum of the AgNPs exhibited a characteristic absorption band at 3450 $cm^{-1}$ (O–H stretching vibration), indicating a high level of interaction with compounds containing OH, thus showing that the hydroxyl-containing compounds may have a significant role in stabilizing the nanoparticles. The relationship and changing intensity of this broad H–O peak between the extract and AgNPs indicate hydrogen bonding between the nanoparticle surface and capping biomolecules. Meanwhile, the bands that were initially at 1127 $cm^{-1}$ and 1620 $cm^{-1}$ showed slight changes and lower intensity, which indicates that the following functional groups were actively involved in the reduction of $Ag^{+}$ ions to $Ag^{0}$ and then absorbed on the surface of the nanoparticle. The loss or reduction in the intensity of some peaks of the plant extract in the AgNP spectrum indicates that phytochemicals were consumed, oxidized, or their structure was altered during nanoparticle preparation. Specifically, polyphenols, flavonoids, and proteinaceous compounds have been reported to donate electrons to silver ions, and the recorded changes in the spectral alterations substantiate their bifunctional role as reducing and capping agents. The remaining features in the AgNP spectrum ensure that these biomolecules are still attached to the nanoparticle surface, which sterically and electrostatically stabilizes them against aggregation [38].

### *3.3 X-Ray Diffraction (XRD)*

The X-ray diffraction (XRD) patterns of the prepared silver nanoparticles (AgNPs) indicate four major diffraction peaks at $2\theta \approx 38.1°$, 44.3°, 64.5°, and 77.4°, which

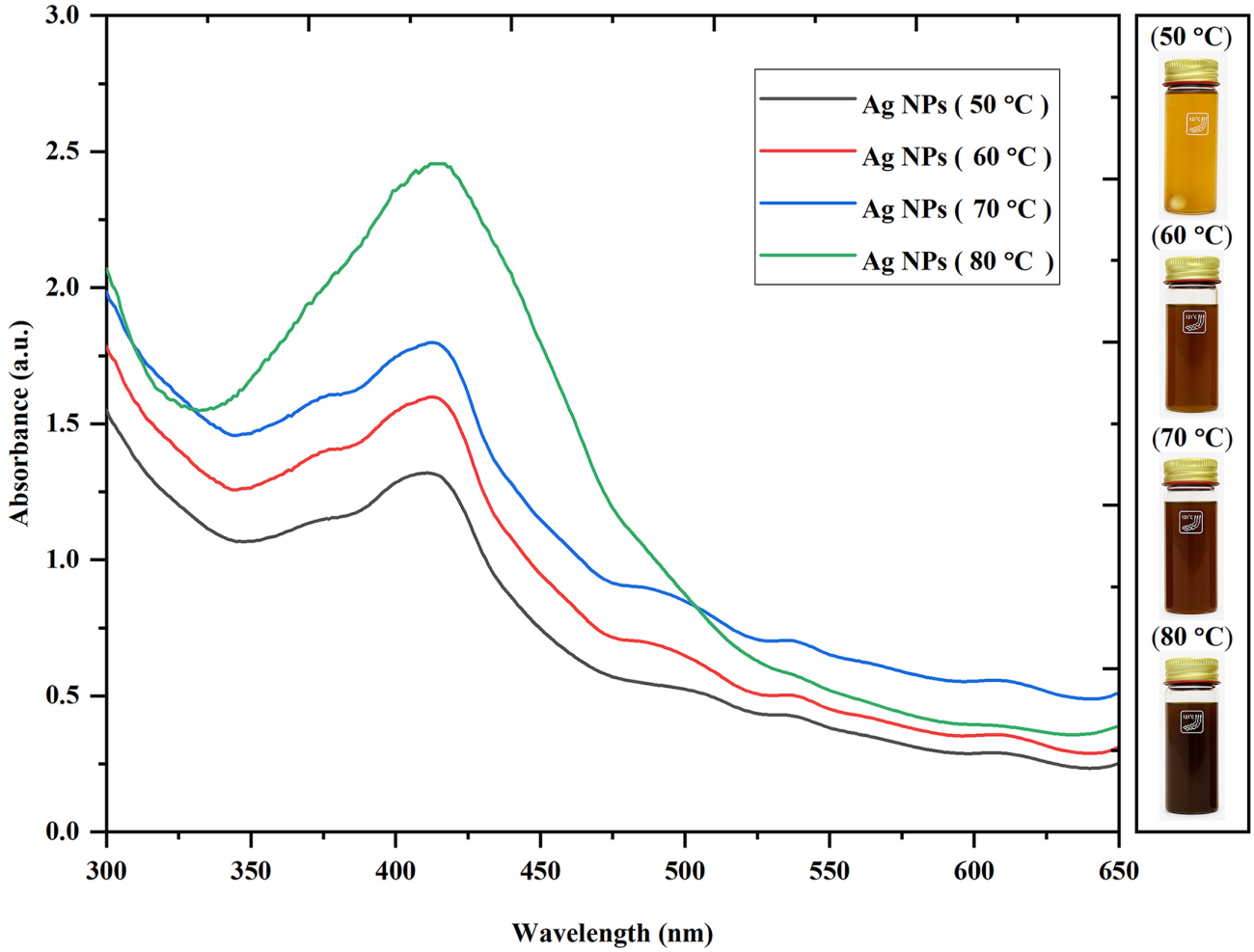


**Fig. 3. Ultraviolet and visible absorption spectra image of silver nanoparticles, 50 °C, 60 °C, 70 °C, 80 °C.**

can be indexed as (111), (200), (220), and (311) crystallographic planes of face-centered cubic (FCC) metallic silver, as shown in Fig. 6. These diffraction characteristics are perfectly in line with the standard JCPDS reference for Ag, which demonstrates the successful production of crystalline metallic silver with no trace of secondary phases. The absence of further strong reflections related to common silver oxides ($Ag_2O$ or AgO) also indicates the purity of the obtained nanoparticles. There is a strong tendency towards the growth in the sharpness and intensity of the peaks as the synthesis temperature increases to 80 °C. The higher the temperature of the sample, the narrower the width of the peak and the more intense the reflections, which indicate that the crystals are more ordered and there are fewer imperfections in the lattice. This tendency is in line with thermally enhanced crystal growth, in which higher temperatures supply the crystal with sufficient energy to improve the atomic arrangement in the metallic lattice [39].

The Scherrer equation [40] was used to estimate the crystallite size based on the most significant reflections of the major (111), (200), (220), and (311) [27]. The theoretical crystallite diameters increased regularly with the synthesis temperature. At 60 °C, the crystallite size values fall within the lower nanometer range, whereas samples prepared at 70 and 80 °C show progressively larger crystalline domains [41]. The considerable growth in the calculated crystallite size at the temperature range of 70–80 °C (Table 1) is due to the increased crystal growth processes thermally catalyzed during the formation of nanoparticles. The movement of silver atoms and clusters within the reaction medium at high temperatures becomes even greater, thus enhancing the diffusion of the atoms and the merging of smaller crystallites into larger ones. This is usually associated with thermally driven crystal growth and Ostwald ripening, where smaller crystal structures dissolve and reappear on larger crystal structures, leading to a reduction in the surface energy and the formation of more thermodynamically stable structures. Consequently, higher synthesis temperatures favored the faster formation of crystallites and higher crystallinity of AgNPs. It is also necessary to mention that the crystallite sizes calculated using the Debye-Scherrer equation are approximate values obtained with reference to the peak broadening of the X-ray diffraction patterns. The computed sizes can contain both contributions of the instrumental broadening and microstrain effects, which were not further decoupled in the given study.

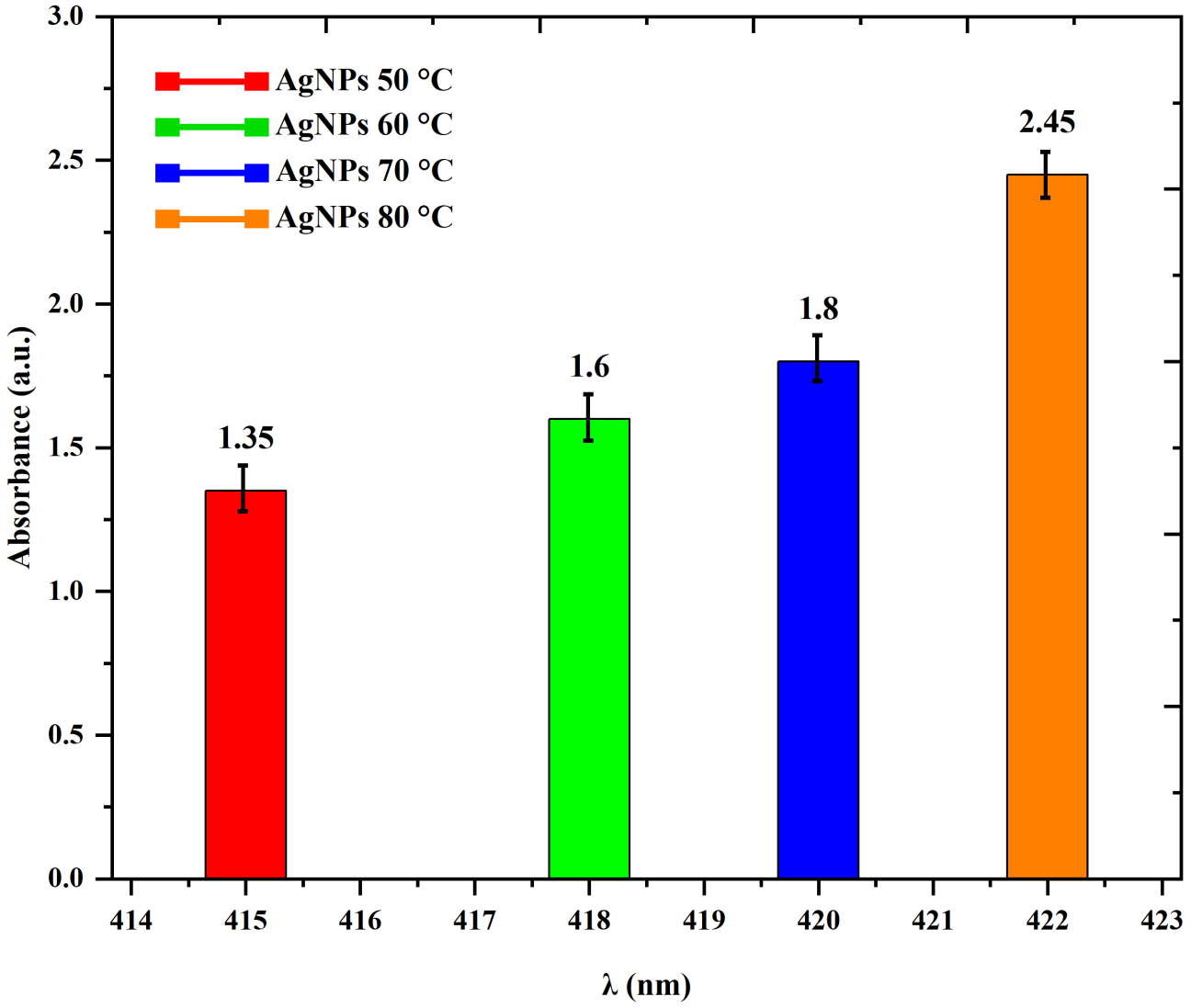


**Fig. 4. A diagram illustrating the absorbance intensity of silver nanoparticles, 50 °C, 60 °C, 70 °C, 80 °C.**

As such, the crystallite sizes reported are supposed to be taken as rough measures of crystallite growth rates, and not the actual dimensions of the particles. However, the systematic sharpening and enhancement of the intensity with increasing temperature are good indicators of the presence of temperature-dependent crystallite growth in the synthesized AgNPs [42,43].

Table 1 shows the approximate size of the crystallites as determined by broadening the peaks and provides a relative tendency with the synthesis temperature.

*3.4 Atomic Force Microscopy (AFM)*

The surface topography, morphology of the particles, and size distribution of the biosynthesized AgNPs deposited as thin films were analyzed using atomic force microscopy (AFM). Fig. 7 shows the representative 3D topographic images and the corresponding particle size histograms of the samples prepared at 70 °C and 80 °C. According to the analysis of the images (Table 2), the main particle sizes in the 70 °C sample were 80–90 nm, and in the 80 °C sample

**Table 1. Measurement of AgNPs size using the Debye-Scherrer's equation.**

| T (°C) | 2θ (deg) | (hkl) | C.S | D (nm) | Intensity (a.u.) |
|---|---|---|---|---|---|
| 60 | 38.1 | 111 | 16.809 | 16.8 ± 1.5 | 98.72 |
| | 44.3 | 200 | 17.155 | 17.1 ± 1.5 | 64.20 |
| | 64.5 | 220 | 18.809 | 18.8 ± 1.6 | 35.41 |
| | 77.4 | 311 | 20.454 | 20.4 ± 1.7 | 25.06 |
| 70 | 38.6 | 111 | 33.618 | 33.6 ± 2.3 | 204.66 |
| | 44.8 | 200 | 34.310 | 34.3 ± 2.3 | 170.13 |
| | 65.0 | 220 | 37.618 | 37.6 ± 2.5 | 141.34 |
| | 77.9 | 311 | 40.908 | 40.9 ± 2.7 | 130.99 |
| 80 | 38.9 | 111 | 84.045 | 84.0 ± 5 | 310.59 |
| | 45.1 | 200 | 86.019 | 86.0 ± 5 | 276.07 |
| | 65.3 | 220 | 94.352 | 94.3 ± 6 | 247.28 |
| | 78.2 | 311 | 102.369 | 102.3 ± 2.7 | 236.93 |

AgNPs, silver nanoparticles; C.S, crystallite size; hkl, Miller indices.

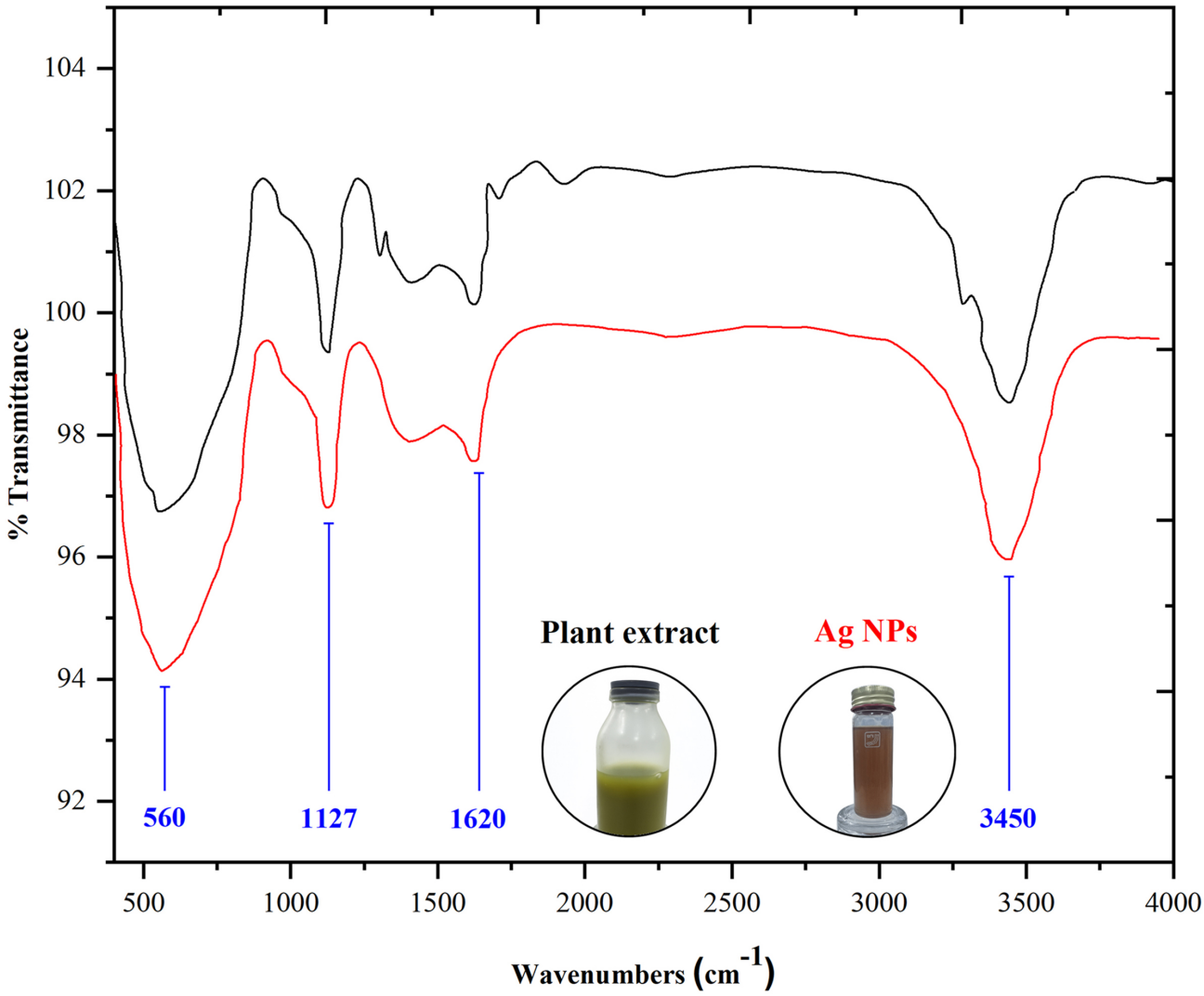


**Fig. 5. FTIR images of silver nanoparticles, *Zanthoxylum fagara* L. Sarg. leaf extract.**

were 93–97 nm (mean diameters of the samples were 85 and 95, respectively). The height maps of the AFM showed a high density of particles, which were roughly hemispherical nanoparticles; that is, there were not long or highly faceted crystals, but discrete protuberances.

**Table 2. Surface roughness rate average diameter of the AgNPs.**

| Sample | D (nm) | Roughness average (nm) | R.M.S (nm) |
|---|---|---|---|
| 70 °C | 80–90 | 7.24 | 16.34 |
| 80 °C | 93–97 | 4.45 | 14.51 |

R.M.S, root mean square.

The quantitative surface roughness parameters measured from the AFM scans revealed that the surface texture changed with the synthesis temperature. The arithmetic average roughness (Ra) value decreased to 7.24 nm (70 °C) and 4.45 nm (80 °C), and the root-mean-square roughness (RMS, Rq) decreased to 16.34 nm and 14.51 nm, respectively. The concomitant growth of the average particle diameter with the reduction in Ra indicates thermally driven particle development and surface rearrangement. The Coarsening of particles (increased mobility of atoms and ions and Ostwald ripening) at elevated synthesis temperatures favors the development of larger, albeit more uniformly distributed surface features that reduce the mean absolute deviation in height (Ra). The slight decrease in RMS compared to Ra suggests that despite the fact that the surface acquires, on average, a smoother appearance, some of the topographic features with high amplitude (taller particles or small agglomerates) maintain a relatively high Rq value [44].

The particle sizes determined by XRD are usually smaller than the particle size because crystallite sizes cannot be compared to the AFM particle size. XRD was used to measure coherently diffracting crystalline domains, whereas AFM was used to measure the entire topographical dimension of nanoparticles, both aggregates and laid on surfaces of phytochemicals. This tends to cause larger apparent particle sizes in AFM without a corresponding de-

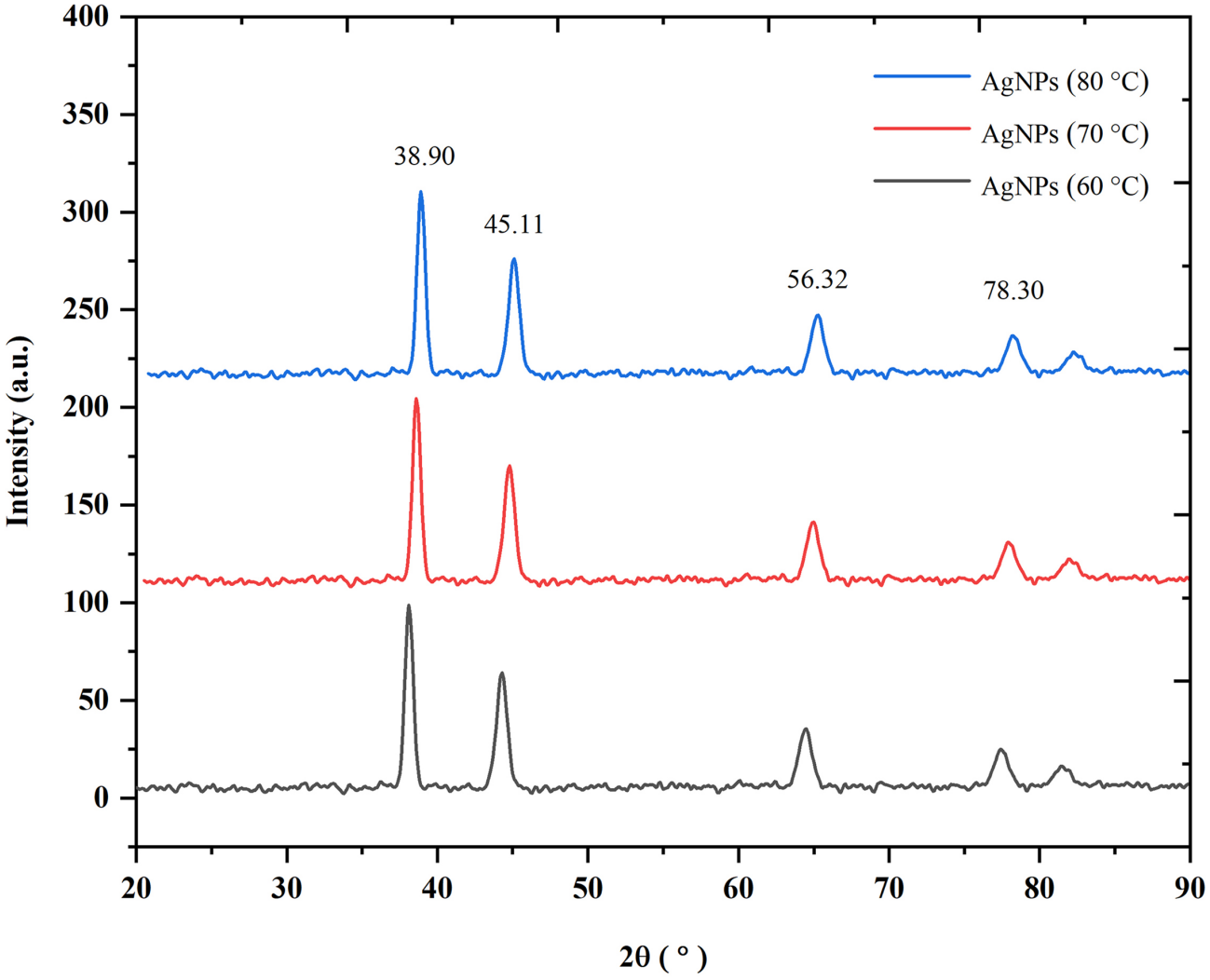


**Fig. 6. XRD images of silver nanoparticles, 60 °C, 70 °C, 80 °C.**

crease in crystallite sizes derived from XRD, which is often observed with green-synthesized metallic nanoparticles [45].

### *3.5 Scanning Electron Microscope (SEM)*

The SEM micrographs presented in Fig. 8 (samples A and B) illustrate the morphological characteristics of Ag nanoparticles synthesized using the aqueous leaf extract of *Zanthoxylum fagara* L. Sarg. under different reaction temperatures (70 and 80 °C) at a constant reaction time of 45 min. The images prove that temperature is an important factor in controlling the size of nanoparticles, their uniformity, and the level of agglomeration.

The sample was taken at 70 °C, as shown in Fig. 8A, and the nanoparticles were mainly spherical and slightly irregular in shape with a fairly broad size distribution. This low reaction temperature results in slower nucleation kinetics, facilitating the development of nanoparticles of different sizes. Moderate aggregation was observed, probably because the reduction of $Ag^{+}$ ions by phytochemicals was not complete, and the stabilization capacity of phytochemicals at this temperature was limited [46]. A significant change in the uniformity of the particles was observed in Fig. 8B at 80 °C. The nanoparticles had a more definite spherical morphology with less variability in size. Increased kinetic energy accelerates the nucleation process at this temperature but allows for controlled growth, which creates a more homogeneous dispersion. The agglomeration level was lower than that in sample A, indicating that the plant-derived biomolecules better capped the nanoparticles, as the plant-derived biomolecules do. This analysis using SEM indicated that the temperature of the synthesis had a strong effect on the morphology and dispersion of the biosynthesized Ag nanoparticles [47].

### *3.6 Photocatalytic Degradation of Methylene Blue*

A rapid reduction in the characteristic absorption peak of methylene blue (MB) at 660 nm was observed with irradiation time (5 to 60 min) in the presence of biosynthesized *Zanthoxylum fagara* L. Sarg. nanoparticles. A high concentration of MB molecules produces a strong and distinct absorption band during photocatalytic activity, which grad-

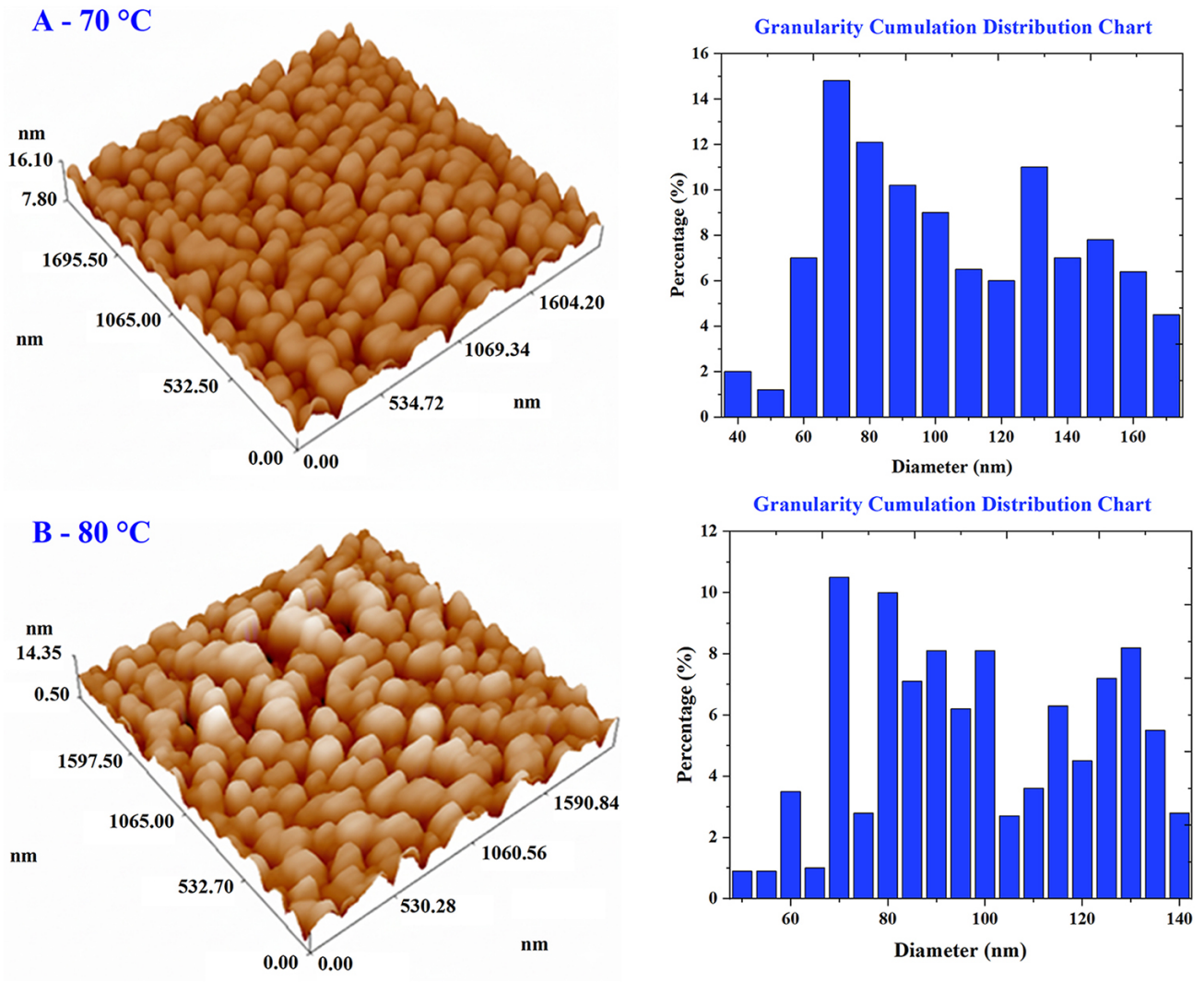


**Fig. 7. AFM images of AgNPs**. (A) 70 °C, (B) 80 °C.

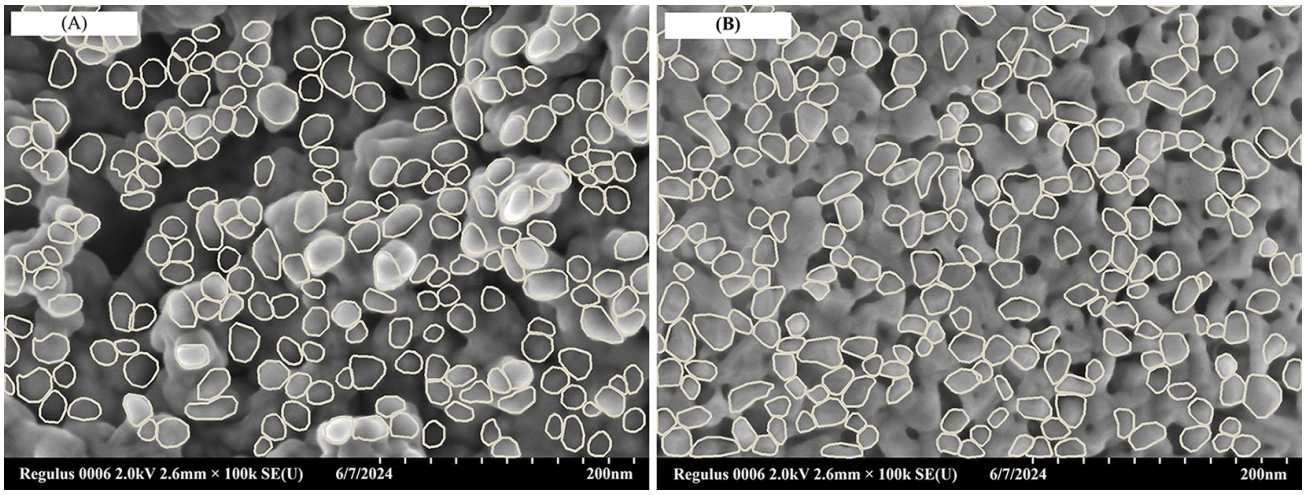


**Fig. 8. SEM images of AgNPs shape, size, and distribution**. (A) 70 °C, (B) 80 °C. Scale bar = 200 nm.

ually diminishes with continued light irradiation upon further irradiation (after 10–20 min), indicating partial degradation that can be easily observed through its decreasing intensity [48]. When the irradiation time is longer (25–45 min), there is a strong suppression of the absorption peak, which is known to be a result of the increased photocatalytic performance of the nanoparticles due to the effective creation of electron–hole pairs on the surface of the

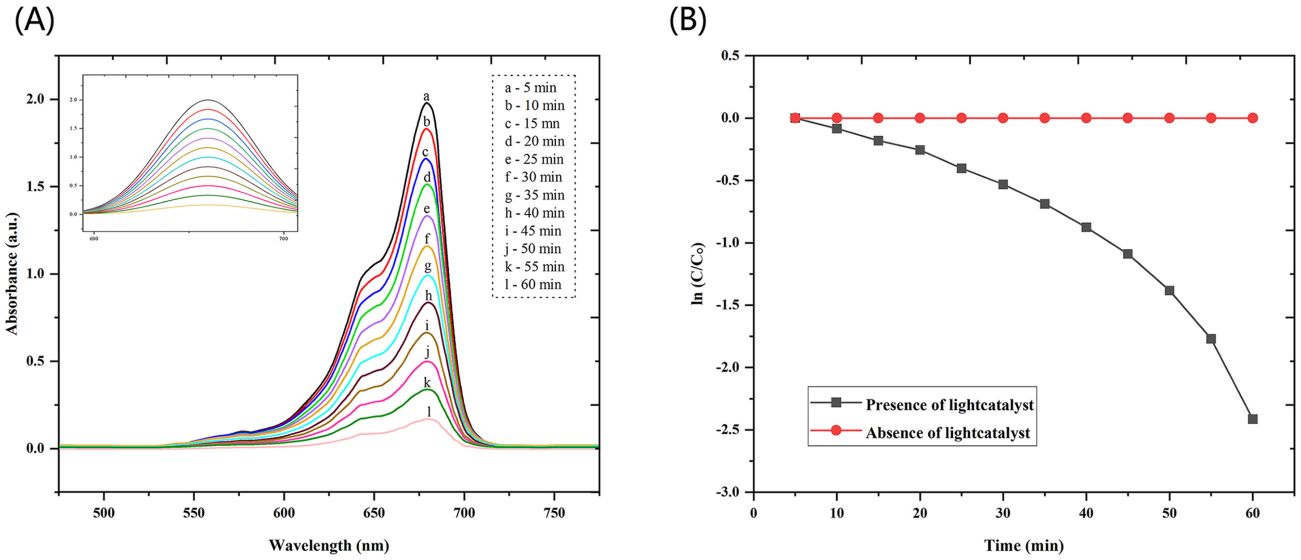


**Fig. 9. Photocatalytic degradation of solutions containing methylene blue via silver nanoparticles**. (A) Extinction spectra of degradation of MB with AgNPs. (B) Degradation kinetics.

nanoparticles. These charge carriers undergo redox reactions, leading to the formation and aggressive attack of MB dye molecules in the decomposition of redox species, such as hydroxyl radicals and superoxide ions. At additional irradiation times above 45 min, a small remnant peak was obtained, indicating that most of the dye molecules had oxidatively broken down. This is evidenced by the fact that the absorption band is significantly reduced by 60 min, indicating the high photocatalytic efficiency of *Zanthoxylum fagara* L. Sarg. nanoparticles, in which most of the MB molecules are destroyed, as shown in Fig. 9 [49]. Recent research has highlighted the need to test photocatalysis systems under realistic environmental conditions to determine their feasibility in a more effective way. The next step in this research should be to investigate the stability, recyclability, and activity of catalysts in a complex wastewater matrix to more accurately assess the environmental viability of this system [50].

This activity is evidence of the high level of interaction between dye molecules and phytogenic nanoparticles because of their nanoscale size, high surface area, and plant-based functional groups that serve as electron mediators present on them. This phenomenon is characterized by a continuously decreasing spectral decay curve of an effective mineralization path, indicating that the biosynthesized nanoparticles are effective under experimental conditions. In general, the catalytic activity of nanoparticle-based systems is pre-evaluated by monitoring the photocatalytic degradation of organic dyes by measuring the change in UV–Vis spectroscopy. However, recent research has indicated that photocatalytic reactions cannot be fully assessed without additional analyses, such as the determination of the nature of intermediates, experiments to trap reactive oxygen species (ROS), and mineralization (e.g., TOC analysis) [49].

Although the present results show that the biosynthesized Ag nanoparticles have good photocatalytic potential for the degradation of methylene blue, certain feasible aspects should be considered. The experiments in controlled laboratory settings using a model dye solution, which is not always reflective of actual wastewater systems. Although the green approach of synthesis using plant extracts would reduce the number of toxic reagents used, the overall sustainability analysis would entail further analyses such as the reusability of the catalysts, toxicity, and life cycle analysis. Recent studies have emphasized that photocatalysis systems should be tested in real environments to determine their feasibility. The second move in this study should be to examine the stability, recyclability, and activity of catalysts in a complicated wastewater mixture to better determine the environmental friendliness of this system [51].

## 4. Discussion

The results indicated that the synthesized AgNPs exhibited significant photocatalytic activity for dye degradation. The higher activity can be ascribed to the small size and large surface area of the prepared nanoparticles, which allowed an increased number of active surface sites for the photocatalytic process. Furthermore, the phytochemical components from the plant extract might have played a role in protecting the AgNPs and enhancing the charge separation efficiency during the photocatalytic process.

The UV–Vis and structural characterization results indicated the successful preparation of crystalline AgNPs with good dispersion. The optical performance was related to the surface plasmon resonance (SPR) phenomenon, which is essential for improving light absorptivity and photocatalytic activity. In addition, the method applied here is also beneficial over other established chemical preparation methods, as it is environmentally friendly.

These biosynthesized AgNPs solutions have competitive dye removal efficiency with the previously reported studies under relatively simple preparation conditions. Green synthesis approaches can provide cost-effective and sustainable nanomaterials for wastewater treatment applications.

*Limitations*

The synthesized AgNPs showed good photocatalytic activity for the removal of dyes, but there were some shortcomings. The present study concentrated mainly on the efficiency of apparent decolorization without studying complete mineralization and identification of intermediate degradation products. Furthermore, the long-term stability and the recyclability of the nanoparticles that were synthesized were not explored. Future studies should, therefore, focus on the quantum efficiency, reusability, and real wastewater applicability, further confirming the environmental potential.

## 5. Conclusions

A green method for synthesizing Ag nanoparticles was performed using *Zanthoxylum fagara* L. Sarg. through the use of *Zanthoxylum fagara* L. Sarg. leaf extracts at different temperatures. Characterization suggested that larger, less homogeneous, and highly crystalline nanoparticles with better surface properties were preferentially accumulated with an increase in the synthesis temperature. Such structural improvements were connected to the increased efficiency of photocatalytic degradation of methylene blue in the laboratory, which proves the significance of temperature in the creation of nanoparticles. Despite these findings suggesting the possibility of using biogenic AgNPs in photocatalytic reactions, the recovery of catalysts, stability, leaching of silver, and possible secondary pollution should be addressed before the applications can be realized during environmental or wastewater treatment.

## Availability of Data and Materials

The data set created and analyzed during this study is available from the author in charge upon reasonable request.

## Author Contributions

Researcher LSA designed the study and developed its theoretical and practical plan and graphed the data obtained using Origin software. RTK conducted the practical part of the research and documented the steps in detail. IHA wrote and edited the initial draft of the manuscript, collecting and documenting scholarly references, participating in the analysis of the study samples, and formatting the references using Mendeley software. All authors contributed to editorial changes in the manuscript. All the authors have read and approved the final manuscript. All authors have participated sufficiently in the study and agreed to be accountable for all aspects of the work.

## Ethics Approval and Consent to Participate

Fresh leaves of *Zanthoxylum fagara* L. Sarg. were collected from a cultivated farm in Hit, Anbar Governorate, Iraq, with permission of the farm owner, in compliance with national and local regulations. A reference sample was deposited in the herbarium of Anbar University (Ramadi, Iraq) and identified by (Desert Studies Center, Ramadi, Iraq). Laith Saleh Alhiti provided the data for the experiment and study design.


## Acknowledgment

Not applicable.

## Funding

This research received no external funding.


## Conflicts of Interest

The authors declare no conflicts of interest.

## References


[1] Beck F, Loessl M, Baeumner AJ. Signaling strategies of silver nanoparticles in optical and electrochemical biosensors: considering their potential for the point-of-care. Mikrochimica Acta. 2023; 190: 91. https://doi.org/10.1007/s00604-023-05666-6

[2] Ivanišević I. The Role of Silver Nanoparticles in Electrochemical Sensors for Aquatic Environmental Analysis. Sensors (Basel, Switzerland). 2023; 23: 3692. https://doi.org/10.3390/s23073692

[3] Chugh D, Viswamalya VS, Das B. Green synthesis of silver nanoparticles with algae and the importance of capping agents in the process. Journal, Genetic Engineering & Biotechnology. 2021; 19: 126. https://doi.org/10.1186/s43141-021-00228-w

[4] Srinivasan LV, Rana SS. A critical review of various synthesis methods of nanoparticles and their applications in biomedical, regenerative medicine, food packaging, and environment. Discover Applied Sciences. 2024; 6: 371. https://doi.org/10.1007/s42452-024-06040-8

[5] Alhiti LS, Hashim EH, Abdullah FH. Green Methods for Gold Nanoparticle Synthesis: Properties, Characterization, and Diverse Applications - Review Article. Humanities and Natural Sciences Journal. 2025; 6: 249–265. https://doi.org/10.53796/hnsj63/12

[6] Alhiti LS, Jawad RA, Abd Alwaahed RA, Sobhi HM. Study of the Effect of Thin Layer Thickness on the Structural Properties of Copper Phthalocyanine (CuPc) Films Prepared by Vacuum Thermal Evaporation Method. Al-Kitab Journal for Pure Sciences. 2024; 8: 81–91. https://doi.org/10.32441/kjps.08.01.p8

[7] Rupanshi, Kumar V, Yadav N, Singh D, Beniwal V, Chhabra J, et al. Biogenic Silver Nanoparticles as Next-Generation Green Catalysts for Multifaceted Applications. Transactions of Tianjin University. 2025; 31: 145–178. https://doi.org/10.1007/s12209-025-00427-3

[8] Younis AAQ, Alhiti LS, Naeem GA, Musa BH, Lateef HR. Preparation of Gold Nanoparticles from E-Waste Using Environmentally Friendly Techniques and Their Optical and Structural Study. Annales de Chimie - Science des Matériaux. 2025; 49: 435–440. https://doi.org/10.18280/acsm.490411

[9] El-Esawy MA, Elsharkawy S, Youssif MM, Tartour AR, Elsharkawy FR, Badr SAS, et al. Recent advances of green nanoparticles in energy and biological applications. Materials Today. 2024; 72: 117–139. https://doi.org/10.1016/j.mattod.2023.12.001

[10] Gao Y, Torrente-Murciano L. Mechanistic insights of the reduction of gold salts in the Turkevich protocol. Nanoscale. 2020; 12: 2740–2751. https://doi.org/10.1039/c9nr08877f
[11] De Berardis B, Marchetti M, Risuglia A, Ietto F, Fanizza C, Superti F. Exposure to airborne gold nanoparticles: a review of current toxicological data on the respiratory tract. Journal of Nanoparticle Research. 2020; 22: 235. https://doi.org/10.1007/s11051-020-04966-9
[12] Dikshit PK, Kumar J, Das AK, Sadhu S, Sharma S, Singh S, et al. Green Synthesis of Metallic Nanoparticles: Applications and Limitations. Catalysts. 2021; 11: 902. https://doi.org/10.3390/catal11080902
[13] Salem SS, Fouda A. Green Synthesis of Metallic Nanoparticles and Their Prospective Biotechnological Applications: an Overview. Biological Trace Element Research. 2021; 199: 344–370. https://doi.org/10.1007/s12011-020-02138-3
[14] Osman AI, Zhang Y, Farghali M, Rashwan AK, Eltaweil AS, Abd El-Monaem EM, et al. Synthesis of green nanoparticles for energy, biomedical, environmental, agricultural, and food applications: A review. Environmental Chemistry Letters. 2024; 22: 841–887. https://doi.org/10.1007/s10311-023-01682-3
[15] Adeyemi JO, Oriola AO, Onwudiwe DC, Oyedeji AO. Plant Extracts Mediated Metal-Based Nanoparticles: Synthesis and Biological Applications. Biomolecules. 2022; 12: 627. https://doi.org/10.3390/biom12050627
[16] Ying S, Guan Z, Ofoegbu PC, Clubb P, Rico C, He F, et al. Green synthesis of nanoparticles: Current developments and limitations. Environmental Technology & Innovation, 2022, 26: 102336. https://doi.org/10.1016/j.eti.2022.102336
[17] Sharma RK, Yadav S, Dutta S, Kale HB, Warkad IR, Zbořil R, et al. Silver nanomaterials: synthesis and (electro/photo) catalytic applications. Chemical Society Reviews. 2021; 50: 11293–11380. https://doi.org/10.1039/d0cs00912a
[18] Zharkova MS, Golubeva OY, Orlov DS, Vladimirova EV, Dmitriev AV, Tossi A, et al. Silver Nanoparticles Functionalized With Antimicrobial Polypeptides: Benefits and Possible Pitfalls of a Novel Anti-infective Tool. Frontiers in Microbiology. 2021; 12: 750556. https://doi.org/10.3389/fmicb.2021.750556
[19] Rani P, Kumar V, Singh PP, Matharu AS, Zhang W, Kim KH, et al. Highly stable AgNPs prepared via a novel green approach for catalytic and photocatalytic removal of biological and non-biological pollutants. Environment International. 2020; 143: 105924. https://doi.org/10.1016/j.envint.2020.105924
[20] Githala CK, Trivedi R. Review on synthesis method, biomolecules involved, size affecting factors and potential applications of silver nanoparticles. Biocatalysis and Agricultural Biotechnology. 2023; 54: 102912. https://doi.org/10.1016/j.bcab.2023.102912
[21] Okagu IU, Ndefo JC, Aham EC, Udenigwe CC. *Zanthoxylum* Species: A Review of Traditional Uses, Phytochemistry and Pharmacology in Relation to Cancer, Infectious Diseases and Sickle Cell Anemia. Frontiers in Pharmacology. 2021; 12: 713090. https://doi.org/10.3389/fphar.2021.713090
[22] Setzer WN, Schmidt JM, Eiter LC, Haber WA. The Leaf Oil Composition of Zanthoxylum fagara (L.) Sarg. from Monteverde, Costa Rica, and its Biological Activities. Journal of Essential Oil Research. 2005; 17: 333–335. https://doi.org/10.1080/10412905.2005.9698923
[23] Ismail M, Akhtar K, Khan MI, Kamal T, Khan MA, M Asiri A, et al. Pollution, Toxicity and Carcinogenicity of Organic Dyes and their Catalytic Bio-Remediation. Current Pharmaceutical Design. 2019; 25: 3645–3663. https://doi.org/10.2174/1381612825666191021142026
[24] Hassaan MA, El-Nemr MA, Elkatory MR, Ragab S, Niculescu VC, El Nemr A. Principles of Photocatalysts and Their Different Applications: A Review. Topics in Current Chemistry (Cham). 2023; 381: 31. https://doi.org/10.1007/s41061-023-00444-7
[25] Jawad RA., Shiltagh N, Aboud LH Watkins MJ. The effect of silver nanoparticles on a mixture of MB-dye/PVA-polymer as determined by absorption and emission spectra measurements. NanoWorld Journal. 2021; 7: 13–21. https://doi.org/10.17756/nwj.2021-087
[26] Jaison JP, Balasubramanian B, Gangwar J, James N, Pappuswamy M, Anand AV, et al. Green Synthesis of Bioinspired Nanoparticles Mediated from Plant Extracts of *Asteraceae* Family for Potential Biological Applications. Antibiotics (Basel, Switzerland). 2023; 12: 543. https://doi.org/10.3390/antibiotics12030543
[27] Güneş S, Ektiren D, Vardin H. Green synthesis and characterization of silver nanoparticles from Gilaburu under varying temperature and pH, with antimicrobial activity and spectral inconsistencies. Scientific Reports. 2025; 15: 38516. https://doi.org/10.1038/s41598-025-00595-1
[28] Alzoubi FY, Ahmad AA, Aljarrah IA, Migdadi AB, Al-Bataineh QM. Localize surface plasmon resonance of silver nanoparticles using Mie theory. Journal of Materials Science: Materials in Electronics. 2023; 34: 2128. https://doi.org/10.1007/s10854-023-11304-x
[29] Asefian S, Ghavam M. Green and environmentally friendly synthesis of silver nanoparticles with antibacterial properties from some medicinal plants. BMC Biotechnology. 2024; 24: 5. https://doi.org/10.1186/s12896-023-00828-z
[30] Ali IH, Saheb HO, Alhiti LS, Al-Fahham AA. Spectroscopy: Types, Principles and Clinical Uses. International Journal of Health & Medical Research. 2024; 3: 469–472. https://doi.org/10.58806/ijhmr.2024.v3i07n08
[31] Alhiti LS, Ali IH. Photodetector Fabrication and Characterization of Gold-Cerium Oxide Nanoparticles for Next-Generation High-Efficiency Devices. Journal of Physics: Conference Series. 2025; 2974: 012033. https://doi.org/10.1088/1742-6596/2974/1/012033
[32] Mcoyi MP, Mpofu KT, Sekhwama M, Mthunzi-Kufa P. Developments in Localized Surface Plasmon Resonance. Plasmonics. 2025; 20: 5481–5520. https://doi.org/10.1007/s11468-024-02620-x
[33] Abdallah RA, El-Borady OM, El-Sayed AF, Fawzy M. A comparative study of chemo- and phytosynthesized silver nanoparticles using Ceratophyllum demersum extract: characterization and biological activities. Biomass Conversion and Biorefinery. 2025; 15: 19013–19029. https://doi.org/10.1007/s13399-025-06718-y
[34] Mandal K, Das D, Bose SK, Chaudhuri A, Chakraborty A, Mandal S, et al. Spectroscopic approach to optimize the biogenic silver nanoparticles for photocatalytic removal of ternary dye mixture and ecotoxicological impact of treated wastewater. Scientific Reports. 2024; 14: 31174. https://doi.org/10.1038/s41598-024-82341-7
[35] Kainat S, Gilani SR, Asad F, Khalid MZ, Khalid W, Ranjha M, et al. Determination and Comparison of Phytochemicals, Phenolics, and Flavonoids in Solanum lycopersicum Using FTIR Spectroscopy. Food Analytical Methods. 2022; 15: 2931–2939. https://doi.org/10.1007/s12161-022-02344-w
[36] Pasieczna-Patkowska S, Cichy M, Flieger J. Application of Fourier Transform Infrared (FTIR) Spectroscopy in Characterization of Green Synthesized Nanoparticles. Molecules (Basel, Switzerland). 2025; 30: 684. https://doi.org/10.3390/molecules30030684
[37] Dugganaboyana GK, Kumar Mukunda C, Jain A, Kantharaju RM, Nithya RR, Ninganna D, et al. Environmentally benign silver bio-nanomaterials as potent antioxidant, antibacterial, and antidiabetic agents: Green synthesis using *Salacia oblonga* root extract. Frontiers in Chemistry. 2023; 11: 1114109. https://doi.org/10.3389/fchem.2023.1114109
[38] Moges W, Misskire Y. Green synthesis, characterization and antibacterial activities of silver nanoparticles using Sida schimperi-

ana Hochst. ex A. Rich (Chifrig) leaves extract. Discover Materials. 2025; 5: 34. https://doi.org/10.1007/s43939-025-00221-x

[39] Gupta P, Ilyas H, Raghav DS, Tomar S. Sustainable synthesis of silver nanoparticles via hordeum vulgare seed extract: catalysis, antioxidant, anti-cancerous and antimicrobial potential. Discover Materials. 2025; 5: 143. https://doi.org/10.1007/s43939-025-00342-3

[40] Nasiri S, Rabiei M, Palevicius A, Janusas G., Vilkauskas A, Nutalapati V, et al. Modified Scherrer equation to calculate crystal size by XRD with high accuracy, examples Fe2O3, TiO2 and V2O5. Nano Trends. 2023; 3: 100015. https://doi.org/10.1016/j.nwnano.2023.100015

[41] Mohammed AH, Ali AM, Awf MB, Abdulwahid RAA, Saleh L, Naeem GA. Green Synthesis and Characterization of ZnO and MgO Nanoparticles Using Chamomile Extract. Sana'a University Journal of Applied Sciences and Technology. 2026; 4: 1825–1830. https://doi.org/10.59628/jast.v4i3.2488

[42] Han Y, Zhu L, Zhang X, Wang K, Sha D, Chen Q, et al. Green synthesis, characterization, and anticancer activity of silver nanoparticles via *Pulsatilla koreana* root extract. Frontiers in Nutrition. 2026; 13: 1746280. https://doi.org/10.3389/fnut.2026.1746280

[43] Bashir N, Afzaal M, Khan AL, Nawaz R, Irfan A, Almaary KS, et al. Green-synthesized silver nanoparticle-enhanced nanofiltration mixed matrix membranes for high-performance water purification. Scientific Reports. 2025; 15: 1001. https://doi.org/10.1038/s41598-024-83801-w

[44] Rüzgar Ş, Eratilla V. The Effect of Deposition Temperature on Structural, Morphological, and Dielectric Properties of Yttria-Doped Zirconia Thin Films. Sinop Üniversitesi Fen Bilimleri Dergisi. 2024; 9: 44–60. https://doi.org/10.33484/sinopfbd.1369460

[45] Hassanzadeh-Tabrizi SA. Precise calculation of crystallite size of nanomaterials: A review. Journal of Alloys and Compounds. 2023; 968: 171914. https://doi.org/10.1016/j.jallcom.2023.171914

[46] Ibrahim NH, Taha GM, Hagaggi NSA, Moghazy MA. Green synthesis of silver nanoparticles and its environmental sensor ability to some heavy metals. BMC Chemistry. 2024; 18: 7. https://doi.org/10.1186/s13065-023-01105-y

[47] Ansari M, Ahmed S, Abbasi A, Khan MT, Subhan M, Bukhari NA, et al. Plant mediated fabrication of silver nanoparticles, process optimization, and impact on tomato plant. Scientific Reports. 2023; 13: 18048. https://doi.org/10.1038/s41598-023-45038-x

[48] Jadhav V, Dhanwate Y, Raut P, Shinde S, Sawant R, Bhagare A. Efficient photocatalytic methylene blue dye degradation from green-synthesized silver-doped iron oxide ($Ag@Fe_2O_3$) nanostructures. Discover Nano. 2025; 20: 66. https://doi.org/10.1186/s11671-025-04242-6

[49] Pourali S, Amrollahi R, Alamolhoda S, Masoudpanah SM. In situ synthesis of ZnO/g-$C_3N_4$ based composites for photodegradation of methylene blue under visible light. Scientific Reports. 2025; 15: 462. https://doi.org/10.1038/s41598-024-84645-0

[50] Younis SA, Kim K-H. Heterogeneous Photocatalysis Scalability for Environmental Remediation: Opportunities and Challenges. Catalysts. 2020; 10: 1109. https://doi.org/10.3390/catal10101109

[51] Sharma D, Kumar A, Singh N. Optimized conditions for phytoinspired fabrication of silver nanoparticles (AgNPs) and exploring their photo- and chemocatalytic routes of methylene blue (MB) dye degradation. Biomass Conversion and Biorefinery. 2024; 14: 13563–13594. https://doi.org/10.1007/s13399-022-03560-4